Material Limitations involving Nonlinear Damping

(Poster Presentation)

Randall D. Peters
Mercer University Physics

(1) ***Internal friction*** of support structures in a seismometer are the most important, yet largely unstudied source of damping -- ***limits performance*** at low frequencies.

(2) The associated damping, which is called ***hysteretic*** or *structural*, is more complicated than a simple nonlinear form; its complexity is characterized by discontinuities ('jerky' behavior) due to the ***Portevin LeChatelier (PLC) effect*** (stress/strain analogue to the Barkhausen effect in ferrous materials).

Supporting Literature, fields of

I. MICRODYNAMICS:

Research by well-known groups has confirmed the presence of hysteretic complexities in

(i) **large-scale structures--NASA** (c.f. Research Associate Programs, Jet Propulsion Lab., descr. online at http://www4.nas.edu/pga/rap.nsf/ByTitle/44.40.03.B4154?OpenDocument

(ii) Microelectromechanical Systems (**MEMS**)-- "A Report on the Emerging Field of Microdynamics**",** *NSF Sponsored Workshop on Structured Design Methods for MEMS***,** (online at http://www.design.caltech.edu/NSF_MEMS_Workshop/bib.html)

II. MESODYNAMICS:

As used by Peters in relation to mechanical oscillators--
Influence of anelasticity on mechanical oscillators -- energies near 10^{-11} *J* .
Especially important to **low frequency** seismometry.

Studies of Mesodynamics

EXPERIMENT :

Publications are mainly e-print -- two major summaries:

(1) Peters, R., "***Damping Parts I and II", Vibration and Shock Handbook***, CRC Press, C. deSilva ed., Univ. British Columbia (in press).

(2) Peters, R., "***Friction at the Mesoscale"***, submitted to Contemporary Physics, ed. Peter Knight, Imperial College, London.

(Online information at http://physics.mercer.edu/petepag/nonlin.htm)

THEORY (work of B. Holian, LANL):

(1) ***"Mesodynamics from atomistics: a new route to Hall-Petch"***

(2) ***"Formulating mesodynamics for polycrystalline materials"*** , Europhys. Lett., Vol. 64 No. 3 (November 2003).

Even a pendulum with short period (near 1 s for these curves) dissipates significant energy through internal friction, with air being more important for the light pendulum.

(Graphs of decay time (reciprocal damping coeff.) vs air pressure)

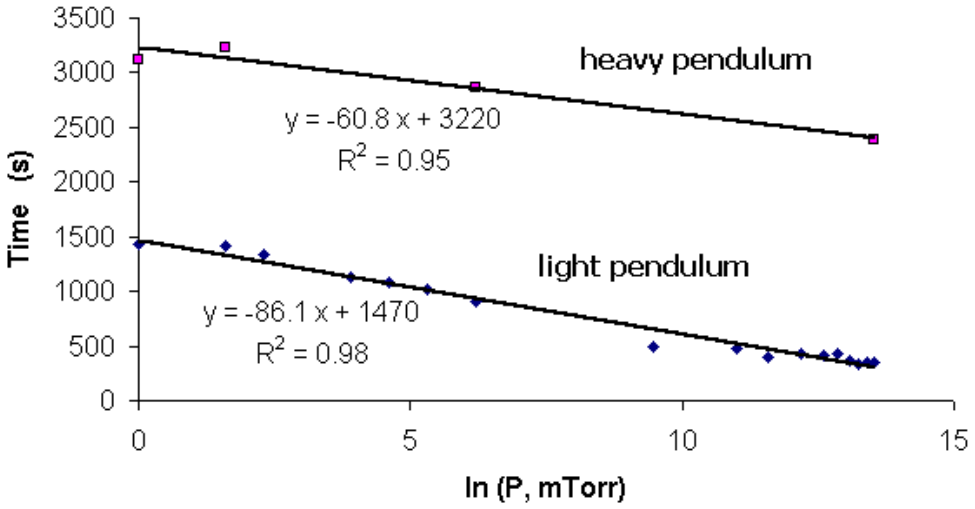

Figure 1. Illustration of the importance of internal friction to the damping of even short-period pendula.

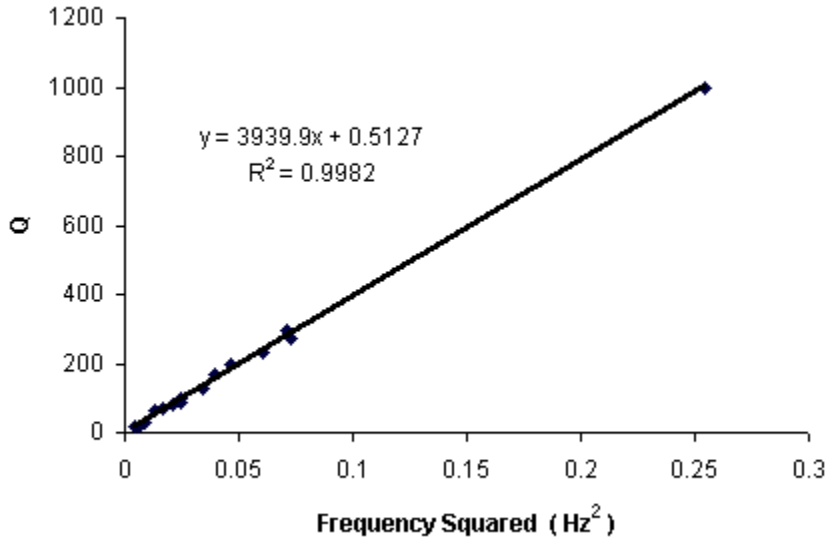

Figure 2. Hallmark of hysteretic damping is Q proportional to frequency squared. (Linear viscous damping requires that Q be proportional to frequency to the first power). The present data was generated with a physical pendulum.

Gunar Streckeisen obtained the same Q vs freq. square dependence for a LaCoste vertical seismometer during his graduate research (data supplied by Erhard Wielandt).

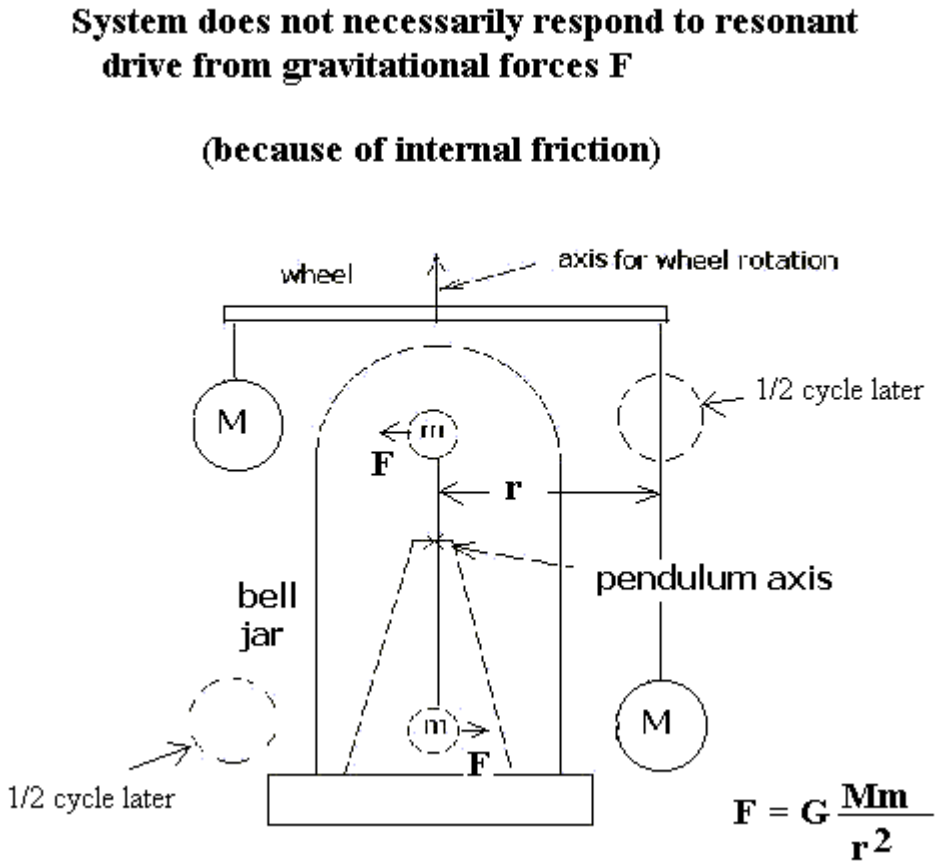

Figure 3. Example of a system (Cavendish-like) in which the 'granular' features of internal friction disallow a meaningful estimate of the Newtonian constant G.

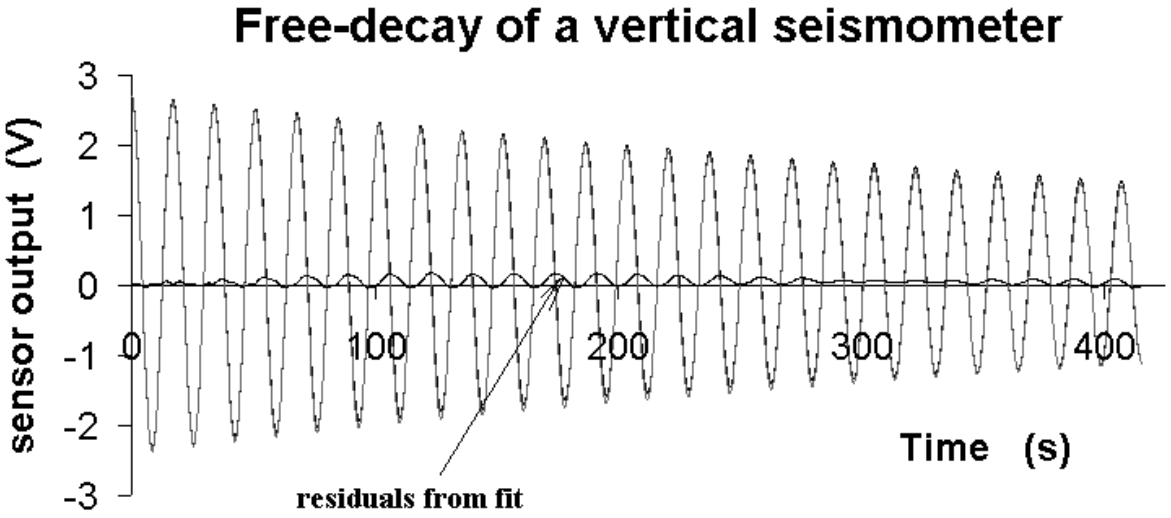

Figure 4. The residuals (from comparison of experiment with conventional theory) show phase noise due to nonlinear (hysteretic) damping. This data was generated with a Sprengnether (LaCoste spring) instrument.

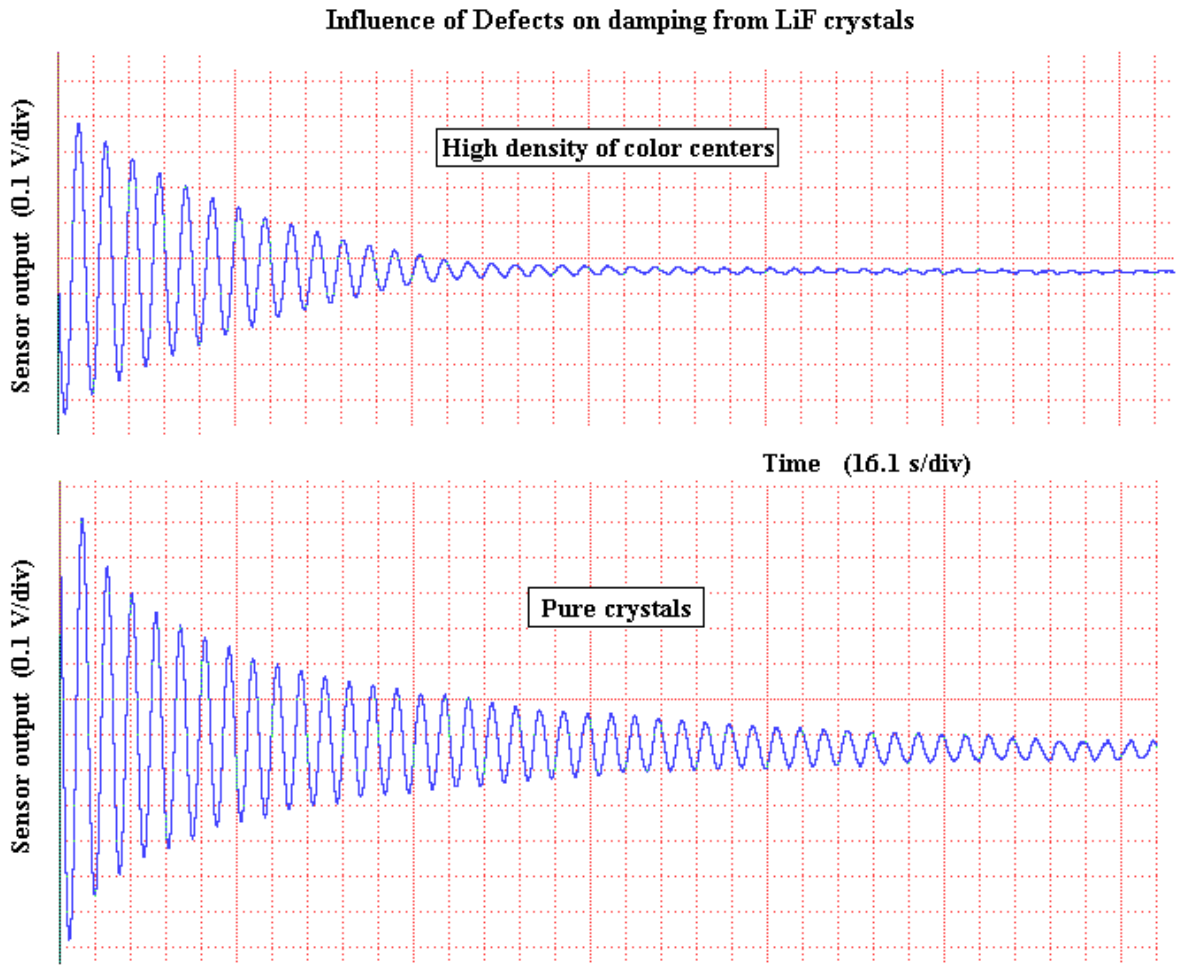

Figure 5. Crystalline defects (here color-centers from gamma irradiation) cause increased internal friction damping. For these free-decays, the crystals were placed, as a pair, under the knife edges of a physical pendulum.

Internal friction is related to creep

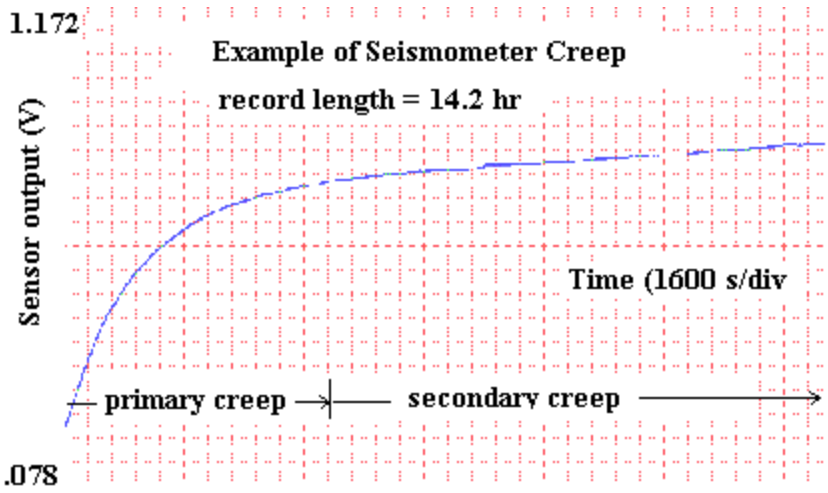

Figure 6. If the state of an instrument is dramatically altered (in this case moved), it can show both primary and secondary creep before it stabilizes. The total vertical travel of the mass in this case was about 1/4 mm during the 14.2 h.

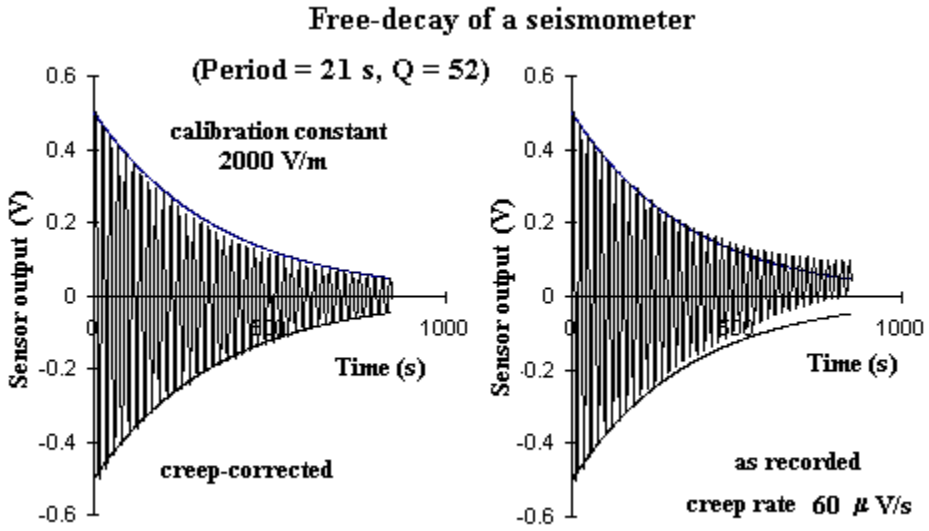

Figure 7. Even after stabilizing, large disturbances usually result in creep. The secular offset in the mean position with time (right curve) has been subtracted out to yield the corrected (left) curve.

Internal friction processes occur at the mesoscale and are not necessarily continuous (smooth).

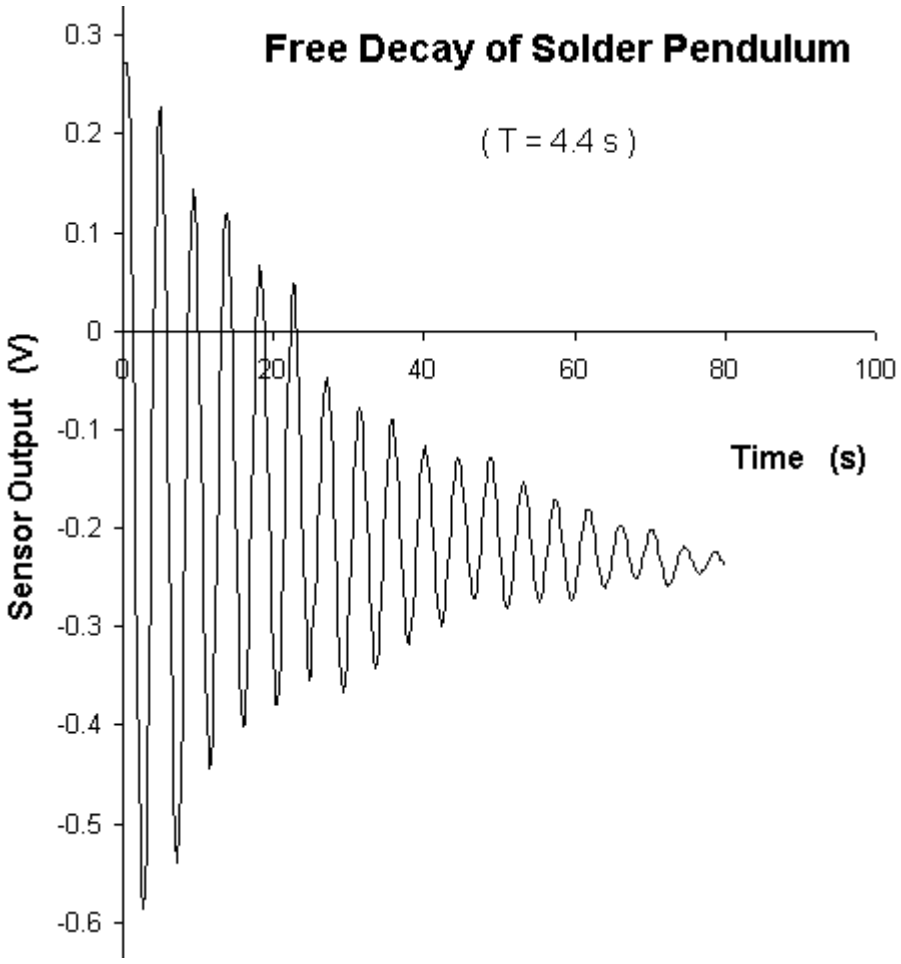

Figure 8. Illustration of 'jerky' behavior due to the Portevin LeChatelier (PLC) effect in a rod pendulum made of solder. Air damping is insignificant here.

Hysteretic damping looks classical at large energies, but at small amplitudes most all pendula show the PLC effect.

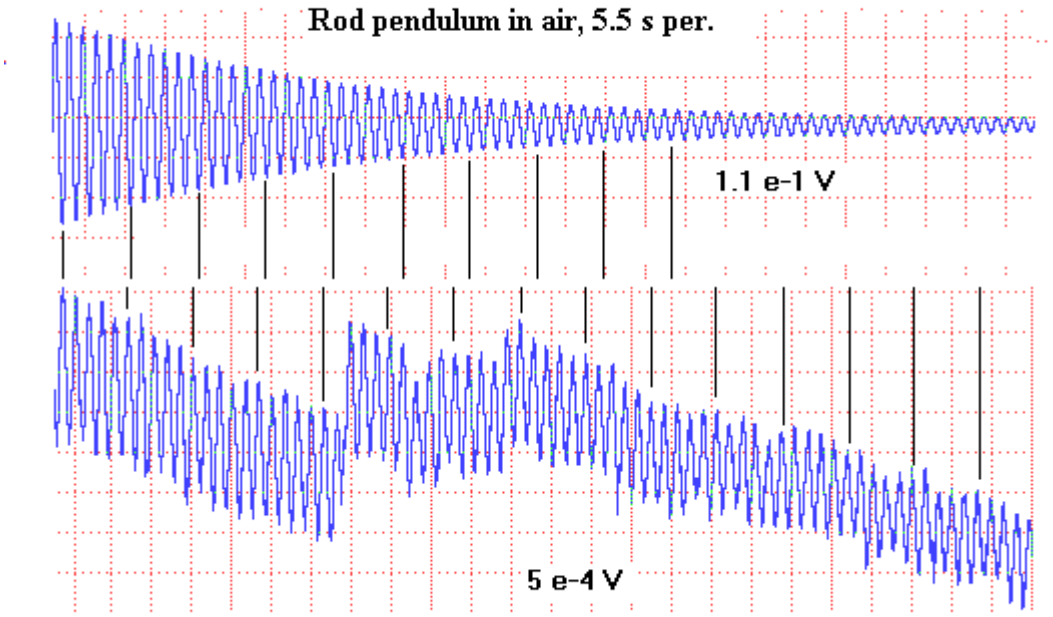

Figure 9. At low levels of the motion, otherwise classical-appearing decays become complex. The voltages are peak-to-peak sensor outputs near the midrange of each trace.

Damping Characteristics

Type	Equation of motion	Damping capacity	Q
Viscous	$\ddot{x} + 2\beta\dot{x} + \omega_0^2 x = 0$	$2\pi\beta\omega A^2 m$	$\frac{\omega}{2\beta}$
Hysteretic (lin. approx.)	$\ddot{x} + \frac{h}{m\omega}\dot{x} + \omega^2 x = 0$	$\pi h A^2$	$\frac{m\omega^2}{h}$
Hysteretic (mod. Coul.)	$\ddot{x} + c_h A \ sgn(\dot{x}) + w^2 x = 0$	$4c_h A^2 m$	$\frac{\pi w^2}{4c_h}$
Coulomb	$\ddot{x} + \frac{f}{m} \ sgn(\dot{x}) + \omega^2 x = 0$	$4fA$	$\frac{\pi m\omega^2 A}{4f}$
Ampl. Dep.	$\ddot{x} + c_f A^2 \ sgn(\dot{x}) + \omega^2 x = 0$	$4c_f A^3 m$	$\frac{\pi\omega^2}{4c_f A}$

Figure 10. Damping capacity, which determines the quality factor Q, is different according to the mechanisms responsible for energy loss.

The modified Coulomb Damping (nonlinear) model developed by Peters is able to describe all of the characteristics indicated in Fig. 10 above.

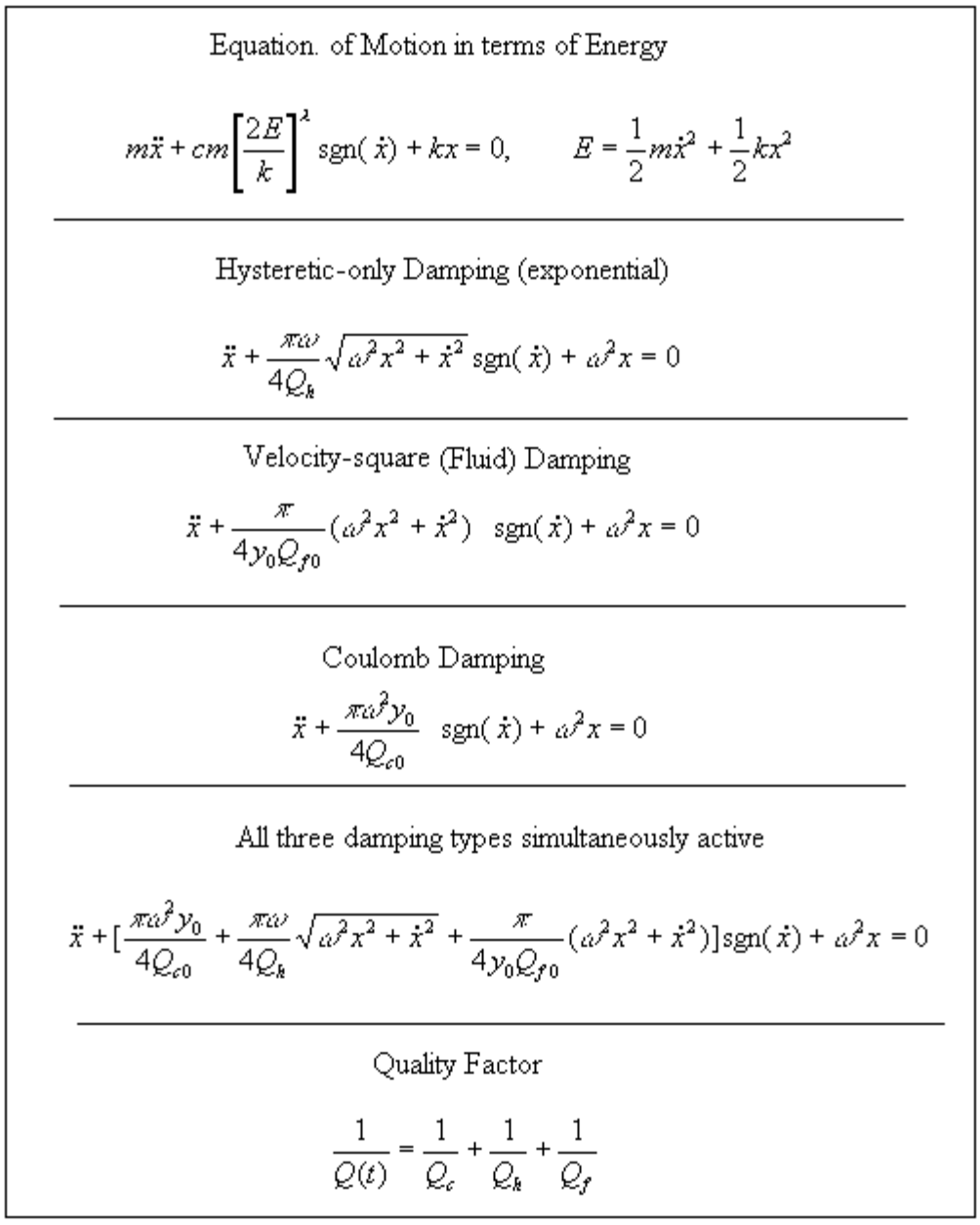

Figure 11. Damping model developed around energy considerations.

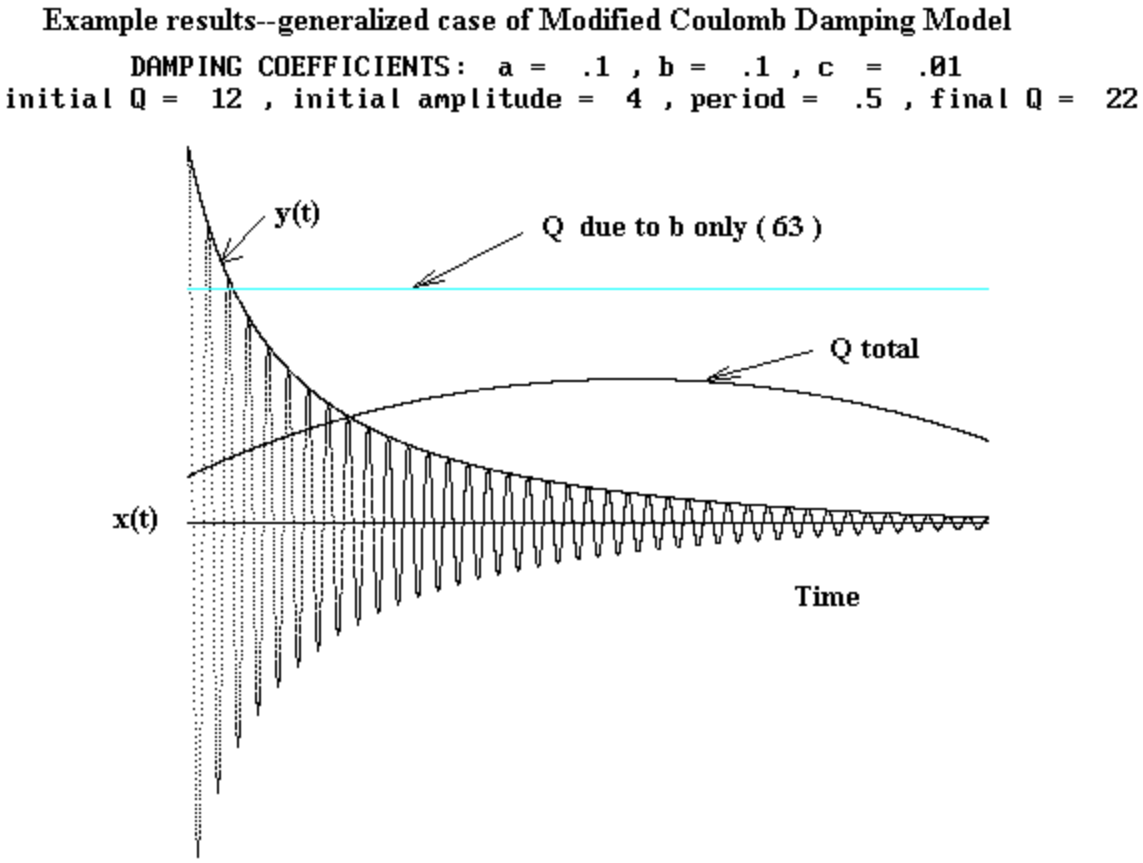

Figure 12. Numerically generated free-decay using the damping model of Fig. 11. The Q varies with time--another hallmark of nonlinear damping.

A power spectrum of the residuals (from experiment fitted to theory) also provides information about nonlinear damping.

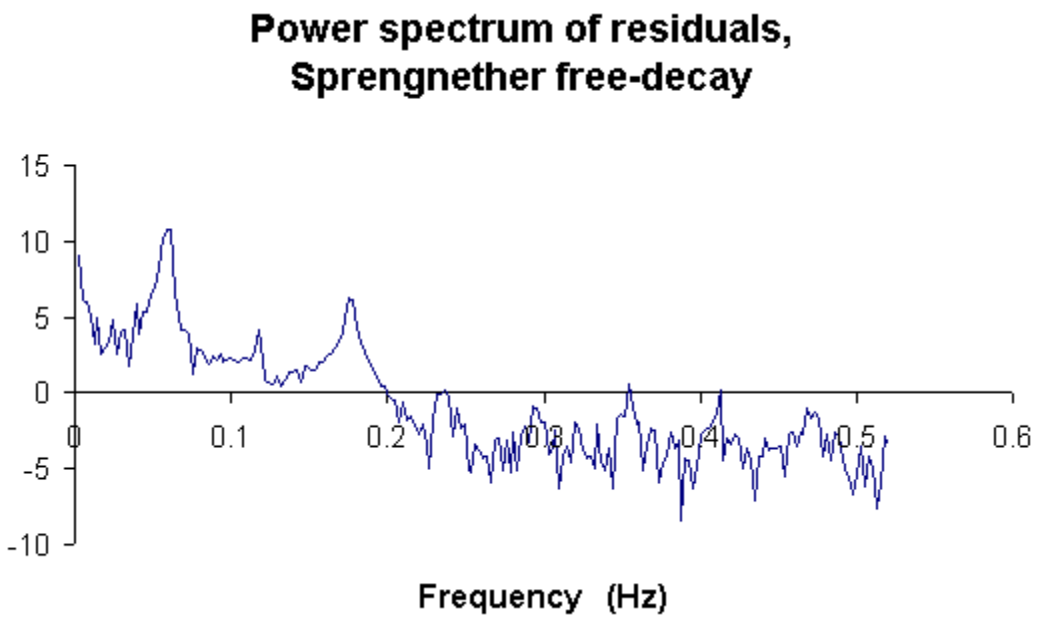

Figure 13. The presence of the third harmonis is evidence for nonlinear (hysteretic) damping of this vertical seismometer.

To fit theory with experiment, it is convenient to work with the turning points y of the motion.

if no damping

$$\dot{E} = \frac{d}{dt}\left(\frac{1}{2}m\dot{x}^2 + \frac{1}{2}kx^2\right) = \dot{x}(m\ddot{x} + kx) = 0, \text{ no friction}$$

with damping (E prop. to y^2 , $\dot{E}$ prop. to ω y · friction force)

$$\dot{E} = -(c_1 + c_2\sqrt{E} + c_3 E)\sqrt{E}$$

equivalent to (c for Coulomb, b for hysteretic, a for fluid)

$$\dot{y} = -c - by - ay^2$$

general solution

with $\alpha = 2ay_0 + b - r, \quad \beta = 2ay_0 + b + r, \quad p = \frac{\alpha}{\beta}\, e^{-rt}$

$$y = \frac{b(p-1) + r(p+1)}{2a(1-p)}$$

special case, c = 0

$$\frac{1}{y} = \left(\frac{a}{b} + \frac{1}{y_0}\right)e^{bt} - \frac{a}{b}$$

special case, a = 0

$$y = \left(y_0 + \frac{c}{b}\right)e^{-bt} - \frac{c}{b} \quad \text{(until y = 0)}$$

Figure 14. Equations used to fit the nonlinear damping model to turning points of the free-decay.

Nonlinear (hysteretic) damping is responsible for the increased noise (1/f) in seismic instruments at low frequencies. This has been demonstrated in both (i) a shape-memory alloy wire and (ii) the Sprengnether vertical seismometer.

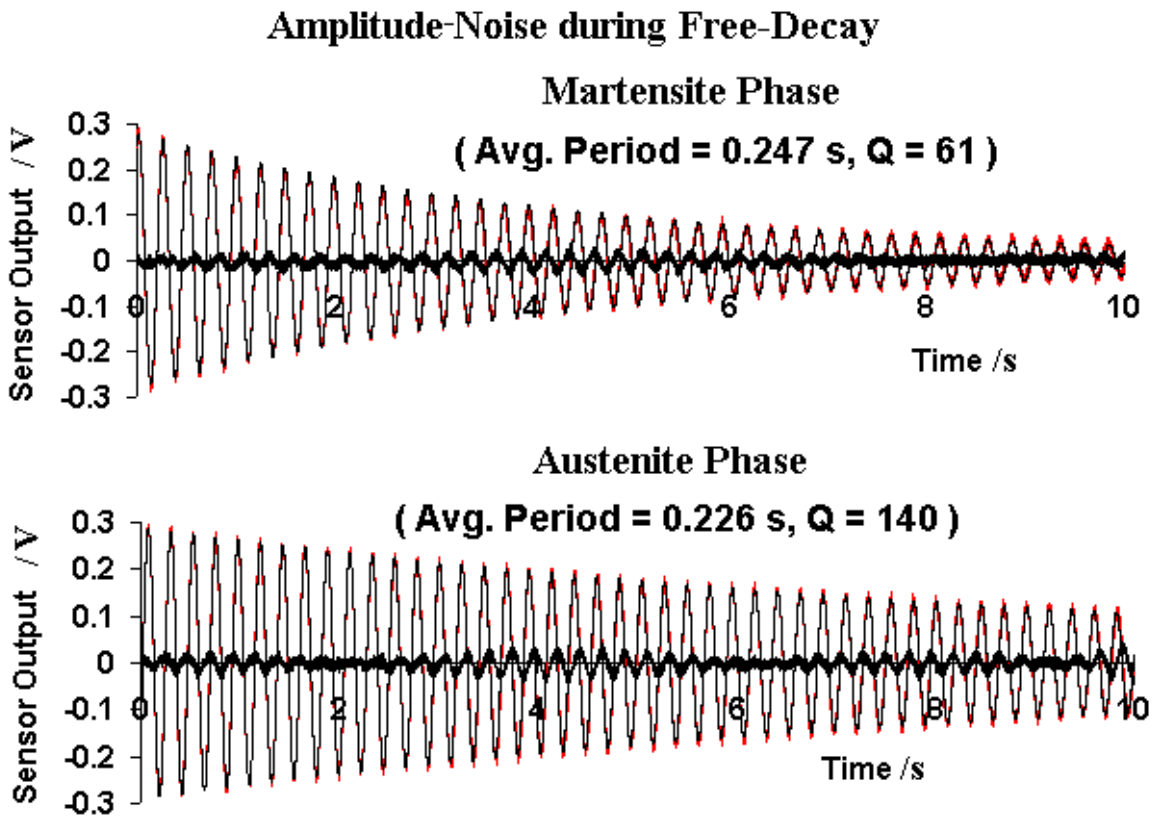

Figure 15. Amplitude noise due to nonlinear damping in a vibratory Nitinol (shape memory alloy) wire. The wire exists in the martensite phase at room temperature; it transforms to the austenite phase at less than 100 C above room temperature.

The residuals can be made smaller by removing the phase noise of Fig. 15, by letting the frequency of oscillation be variable.

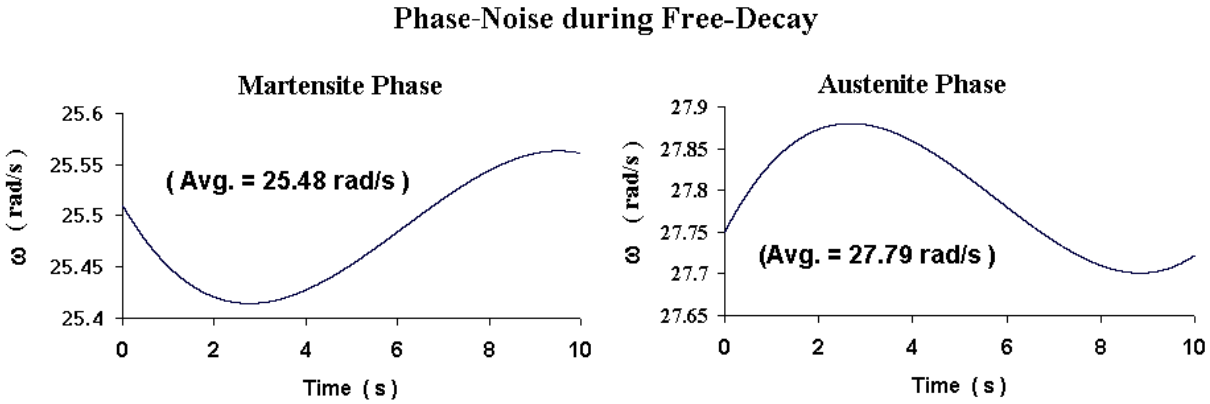

Figure 16. Phase noise corresponding to the free decays of Fig. 15.

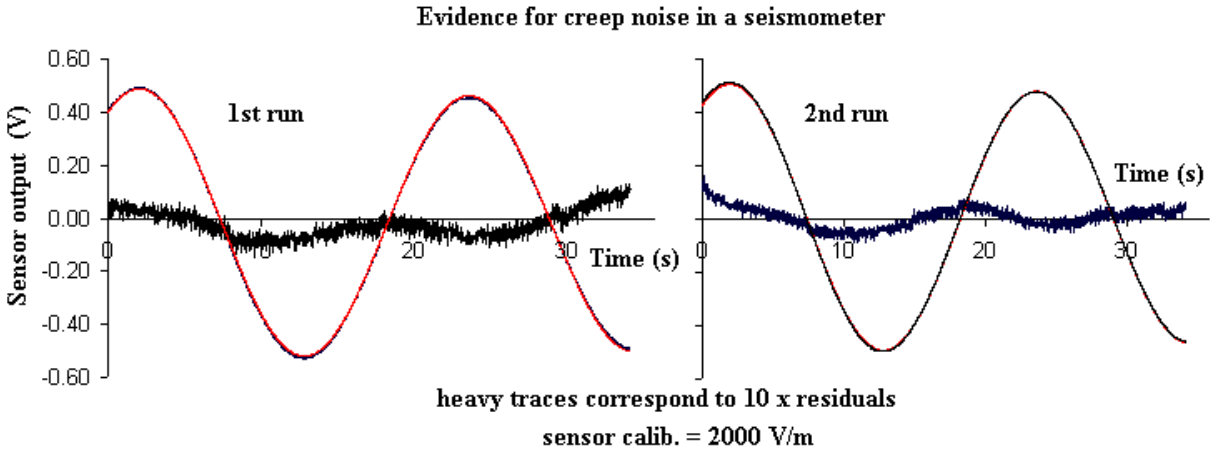

Figure 17. Creep noise due to internal friction decreases as the Sprengnether vertical seismometer stabilizes (as seen by smaller rss variations in the right trace). The noise (1/f) of mechanical type never disappears completely. It is associated with strain/temperature activation of mesoscale defect structures; and it limits the performance of instruments at really low frequencies.